

AMSR-E Monthly Level-3 Rainfall Accumulations
Algorithm Theoretical Basis Document
Thomas T. Wilheit
Department of Atmospheric Science
Texas A&M University
2007

For those 5°x5° boxes that are primarily land, AE_RnGd is simply an average of AE_Rain_L2B; the ensuing discussion pertains entirely to oceanic boxes.

The basis of the retrieval is first to accumulate histograms of the brightness temperatures for 5°x5° boxes for each month. These histograms are converted into monthly total rain rates on the basis of an assumed **form** of the probability distribution function (PDF) for rain.

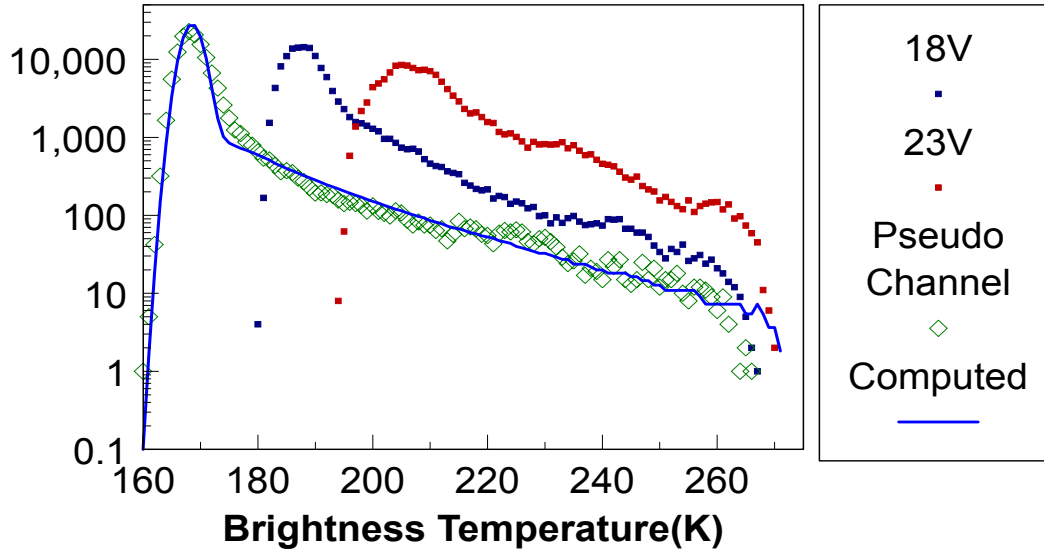
This algorithm was originally developed for application to the SSM/I instrument for the Global Precipitation Climatology Project (GPCP) (Wilheit et al., 1991). The lowest frequency of the SSM/I was 19.35 GHz so that many heavy rain events could not be measured due to saturation. The use of the form of the rain PDF allowed us to fill in the contribution from these heavy rain rates by extrapolation. This algorithm was also modified for application to the Tropical Rainfall Measuring Mission (TRMM) and remains as the 3A11 product (monthly rain totals). The algorithm has proved very stable. It was chosen for the launch version of the AMSR-E monthly rainfall algorithm for this stability since the quality of the instrumental calibration was a large uncertainty in the beginning. It also permits direct comparisons with the long record of SSM/I-based rainfall totals going back to 1987.

The histograms are bounded by latitudes and longitudes divisible by 5 from 60°N to 60°S. Figure 1 shows a typical brightness temperature histogram for the 18.7 and 23.8 GHz channels (both vertically polarized). The histograms are fairly wide due to variability of water vapor over the box during the month. However, if we create another pseudo-channel as a linear combination of these two channels:

$$Tb_{PC} = 2 * Tb_{18V} - Tb_{23V}$$

then the variability is greatly reduced as can be seen in Figure 1; we will use this pseudo-channel as the basis of our rainfall total retrievals.

Histograms of AMSR-E Brightness Temperatures Number of Occurrences



30-35S; 165-170W
July '03

Figure 1

Observed and computed histograms of brightness temperature for two AMSR-E channels and a pseudo channel (2Tb18.7V - Tb23.8V) for a 5°x5° box for a month. The solid curve represents a calculated fit to the linear combination histogram.

Following Kedam *et al.* (1990) rain rates are assumed to be distributed as a Mixed Log-Normal (MLN) over each box.

$$N(r) = (1-P_r) \delta(r) + P_r (2\pi)^{-1/2} r^{-1} \exp(-0.5 * (\ln(r/r_0)/\sigma_{lr})^2)$$

Where $N(r)$ is the probability of a given rain rate, r . P_r is the probability that it is raining at all, $\delta(r)$ is a delta function, r_0 is the logarithmic mean rain rate (when it is raining) and σ_{lr} is the standard deviation of the logarithm of the rain rate when it is raining. In these terms, the time/area average rain rate, R , is given by:

$$R = r_0 P_r \exp(\sigma_{lr}^2/2)$$

Each rain rate, r , be converted into a brightness temperature using an analytic approximation to radiative transfer calculations in the form:

$$T_b = T_0 + (285K - T_0) (1 - \exp(-r/r_c)) - a(r)^{0.5}$$

where r_c (the characteristic rain rate) is given by:

$$r_c = 28.04(\text{mm/h})/(\text{FL}(\text{km}))^{1.13}$$

where FL is the freezing level. The scattering parameter, a , is $5.02 \text{ K}(\text{mm/h})^{-0.5}$. These parameters are computed by fitting this form to radiative transfer calculations for freezing levels ranging from 0.1 to 6km. The value of T_0 (the non-raining brightness temperature) is also expressed this way but we have chosen to let the fitting program solve for T_0 to absorb calibration and modeling errors. The fitted form of T_0 is, however, used in the solution for the freezing level (Appendix II)

For each box we approximate a monthly average freezing level as described in Appendix II. Using this freezing level we convert a MLN distribution of rain rates to a distribution of brightness temperatures—*i.e.* a computed T_b histogram.

The algorithm adjusts the P_r and r_0 parameters of the MLN distribution of rain rate as well as T_0 and $NE\Delta T$ (the instrumental noise) of a computed histogram to match characteristics of the observed histogram. The algorithm fits the mean, variance, and 3rd moment as well as the point on the low brightness temperature end where the histogram value falls to 1/10 of the peak value. Normally, the value of σ_{lr} is left at 1 unless the fitting routine requires unphysical values of P_r . When satisfactory convergence is obtained, the average rain rate is computed per the equation above. For output purposes it is converted to units of mm/day and corrected for rainfall inhomogeneity as described in APPENDIX III. An example of the computed histogram is included in Figure 1.

While the performance of this algorithm has been very good when applied to the SSM/I, TMI and AMSR-E, there is still room for improvement. From the comparison between the observed and computed histograms, it can be seen that while the fit is good, it is by no means perfect. This example is typical, some are better, even much better, and some are worse. One can conclude that the rainfall for this particular box is not quite log-normally distributed. It would be desirable to be able to drop the MLN assumption. Including the 10.7 GHz channel will extend the measurement dynamic range to high enough values that the MLN assumption will no longer be needed to fill in the highest rain rates. Also, the present algorithm uses a single freezing level for the box for the entire month. This is not a bad assumption in the tropics where the freezing level has little variability but at high latitudes it is a definite shortcoming. Lastly, while the AMSR-E has a somewhat worse calibration uncertainty than other similar sensors calibration uncertainty is an issue in all sensors. Solving for T_0 eliminates the calibration error near the non-raining brightness temperature but the uncertainty can be as much as 2K near 280K. By including the lower frequency, we can stay away from these high brightness temperatures and reduce the impact of the calibration uncertainty. An error model based algorithm that uses all of the AMSR-E channels from 10.7 to 36.5 GHz is in the late stages of testing now and is planned to be substituted for or added to this algorithm in the future.

APPENDIX I Radiative Transfer Model

The model used for computing the relationship between rain rate and the observed brightness temperatures is illustrated in Figure I.1. A free parameter of the model is the 0°C isotherm, or Freezing Level. This determines the thickness of the layer of liquid raindrops. We assume a 6.5K/km lapse rate (roughly a global average) so selection of the freezing level determines the entire temperature profile. We assume the relative humidity is 80% at the surface and increases linearly to 100% at the freezing level and above. Thus, the water vapor profile (and precipitable water) is likewise determined by the choice of the freezing level. The rain drops are assumed to be distributed in size according to the Marshall-Palmer (1948) distribution. The absorption and scattering properties are determined from the Mie (1908) theory for dielectric spheres. In addition to the rain drops we assume a token amount of non-precipitating cloud liquid water in the 500 meters below the freezing level. All the water is assumed to be frozen above the freezing level and to have negligible scattering and absorption. Water vapor is assumed to be saturated with respect to ice above the freezing level.

In the absence of scattering, integration of the equation of radiative transfer is trivial. However, scattering makes the integration more difficult as computing the brightness temperature in any direction requires knowledge of the brightness temperature in all other directions. Here we approximate the brightness temperature field in 20 directional steps and solve the equations iteratively. This solution is discussed in Tesmer and Wilheit (1997)

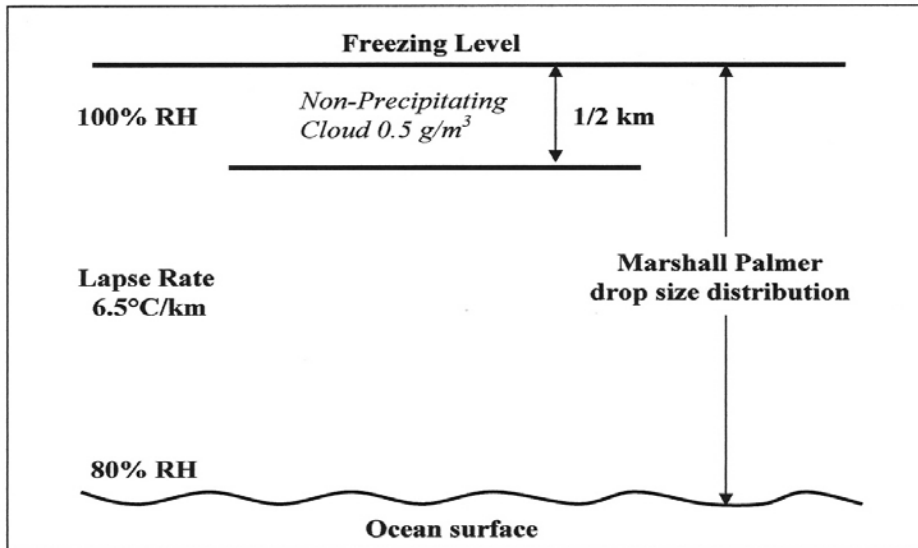


Figure I.1
Pictorial rendition of the model used for radiative transfer in rain.

APPENDIX II Freezing Level Retrieval

As discussed in Appendix I, the precipitable water content (vertically integrated water vapor) freezing level is uniquely determined within the model which, in turn, is a reasonable approximation to the actual atmosphere under raining conditions. This provides the basis for the freezing level retrieval as is illustrated in Figure II.1. Here we have plotted isolines of freezing level while varying the rain rate in a $Tb_{18.7V}$, $Tb_{23.8V}$ space. The left end of the isolines corresponds to zero rain rate. The figure also shows several points from a single scan of AMSR-E data across an oceanic rain feature. Because water vapor absorbs and emits much more at 23.8 than at 18.7 GHz, the contours spread out as a function of freezing level.

Within this algorithm, individual brightness temperatures are not accessible. In order to get a brightness temperature pair, we use the 18.7 and 23.8 GHz histograms to compute the 99th percentile of brightness temperature for each. This pair corresponds to a raining condition in all but the driest boxes. The Tb pair so generated is compared with the freezing level isolines to compute a typical (raining) freezing level for the month. Although it is illustrated graphically, the actual solution is implemented via a lookup table.

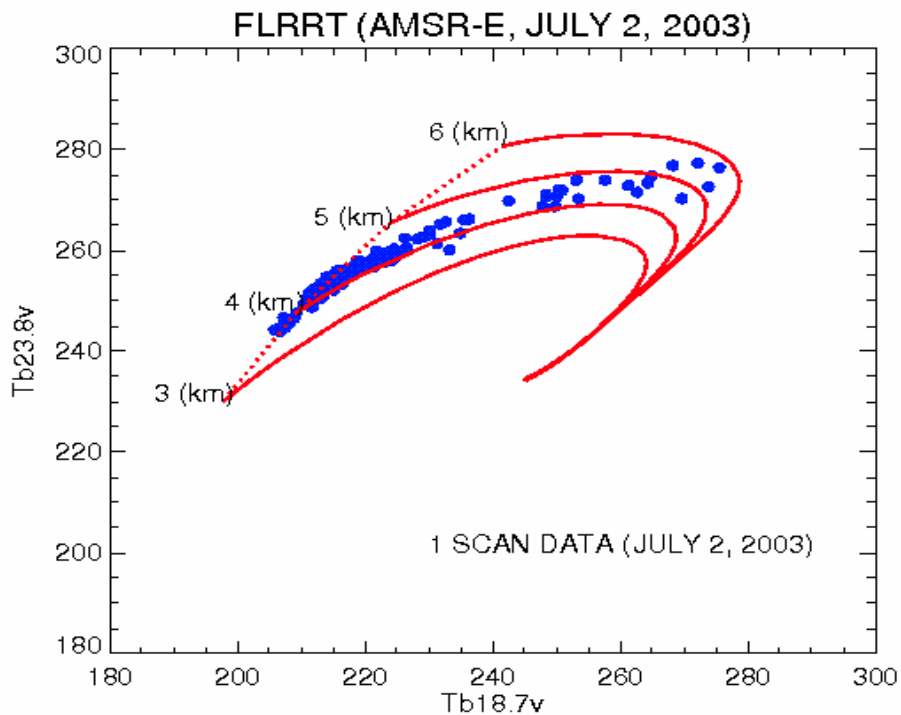


Figure II.1

Freezing Level, Rain Rate, Temperature chart for AMSR-E The dotted line represents zero rain for a variety of freezing levels and the solid lines represent constant freezing levels for as rain rate varies.

APPENDIX III Beam Filling Correction

Spaceborne microwave radiometers typically have fields-of-view on the order of several tens of kilometers at the frequencies relevant to sensing of rainfall over the oceans. Rainfall will completely fill the field of view rarely if ever. Even within the raining part, there will be significant variability in the rainfall intensity. The non-linear nature of the relationship between rain rate and brightness temperature (calculated according to Appendix I) causes a systematic underestimate of the average rainfall over the field-of-view. This is termed Beam Filling Error. For any given field-of-view, in the absence of detailed information about the distribution of rain, a correction is impossible. However, we can generate a correction based on typical rain distributions.

In order to calculate the beam filling correction, we set up a simulation designed to isolate the beam filling error. Wang (1995) used airborne radar data from the TOGA/COARE experiment to drive the simulation. He used the 3 dimensional rain fields from the radar to compute the average rain rate and brightness temperature that would be observed by spacecraft sensors at varying resolutions. The brightness temperature was then used with the computed rain rate-brightness temperature relationship to determine the rain rate that would be retrieved using the relationship at face value. The difference is the beam filling error that must be corrected. He found a relationship among Beam Filling Correction (BFC), spatial resolution and characteristic rain rate r_c (defined in the main body text) as follows:

$$RR_{\text{true}} = \text{BFC} * RR_{\text{face value}}$$

$$\text{BFC} = (1 + (0.478 \ln(S) - 0.687)/r_c)$$

where S is the long dimension of the field of view in km and r_c is the characteristic rain rate in mm/h. For this correction we use the r_c value for the pseudo-channel and the spatial resolution of the 18.7 GHz channel. The monthly total is simply multiplied by BFC.

References

- Kedam, B., L. Chiu, and G. North, 1990: Estimation of mean rain rates: Applications to satellite observations. *J. Geophys Res.* **95**, 1965-1972
- Marshall, T. S. and W. M. Palmer, 1948: The distribution of raindrops with size. *J. Meteorol.*, **5**, 165-166
- Mie, G., 1908: Beiträge zur Optik Trüber Medien, speziell kolloidaler Metalösungen. *Ann. Phys.*, **26**, 597-614.
- Tesmer, J. R., and T. T. Wilheit, 1997: An improved microwave radiative transfer model for tropical oceanic precipitation: *J. Atmos. Sci.* **55** 1674-1688
- Wang, S.A., 1995 Modeling the Beamfilling Correction for Microwave Retrieval of Oceanic Rainfall PhD dissertation, *Dept of Meteorology; Texas A&M University*

Wilheit, T. T., A. T. C. Chang and L. S. Chiu, 1991: Retrieval of monthly rainfall indices from microwave radiometric measurements using probability distribution functions. *J. Atmos. & Oceanic Tech.* **8**, 118-136.